(4)

ERL-0426-TR

AR-004-991

DEPARTMENT OF DEFENCE

DEFENCE SCIENCE AND TECHNOLOGY ORGANISATION

SALISBURY

ELECTRONICS RESEARCH LABORATORY

SOUTH AUSTRALIA

TECHNICAL REPORT

ERL-0426-TR

CO_2 (10.6 μm) LASER TRANSMISSOMETER

S.A. BRUNKER

AR-004-991

DEPARTMENT OF DEFENCE

DEFENCE SCIENCE AND TECHNOLOGY ORGANISATION

ELECTRONICS RESEARCH LABORATORY

TECHNICAL REPORT

ERL-0426-TR

CO_2 (10.6 μm) LASER TRANSMISSOMETER

S.A. Brunker

SUMMARY

A commercially-obtained CO_2 California continuouous-wave (c.w.) laser was used as the infrared (I.R.) emitting component in the construction of a 10.6 μm Laser Transmissometer. This report describes the construction and establishes the performance of the transmissometer. It was found that the laser would oscillate unpredictably between the lower-order transverse electro-magnetic modes, and it was therefore necessary to try to predict pseudo-stationary points in the far diffracted field.

POSTAL ADDRESS: Director, Electronics Research Laboratory,
PO Box 1600, Salisbury, South Australia, 5108.

TABLE OF CONTENTS

LIST OF APPENDICES

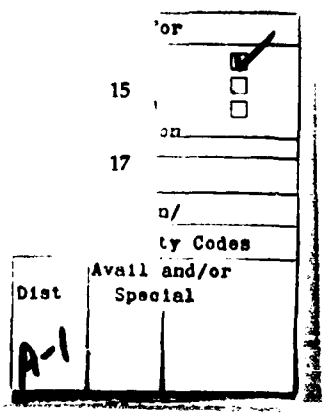

LIST OF FIGURES

1. INTRODUCTION

A Task for the Australian Army was raised to investigate the performance of a number of smoke grenades over the visual, 3 to 5 and 8 to 14 μm wave-bands. The transmissivities of the smokes in the two atmospheric infra-red windows were assessed by using AGA Thermovision thermal imagers. Due to recent research into development of 10.6 μm laser range-finders and radar, it was expedient to construct a CO_2 laser transmissometer so that the transmissivities of smokes and particulates at 10.6 μm could also be investigated.

The commercially-purchased California (82-7500-T) CO_2 laser was found to oscillate at unpredictable times between several of the lower-order transverse modes. Calculations were performed to see if there were points where the intensities in the far diffracted field were time-invariant. These points, if found, were regions in which to place the detector so that a minimum fluctuation in signal would occur when the laser oscillated from one mode to the next.

Once the transmissometer had been built, signal-reproduceability was checked by transmission through normal atmosphere. Aluminium-flake particulate was then introduced, and the transmission-results recorded.

The following report is divided into two main sections. The first details the transmissometer, its application and the associated results. The second details the diffraction theory necessary in obtaining time invariant points in the diffracted field.

2. THE TRANSMISSOMETER

A schematic diagram of the transmissometer's main components is shown in figure 1. The transmissometer comprises components in the near field: laser, beam-expander, aperture, chopper and detector. Those in the far field are: off-axis parabolic condensor and detector.

2.1 Optical components for the near field

2.1.1 Laser

The commercially-obtained CO_2 laser oscillates primarily in the Gaussian TEM_{00} mode at a wavelength of 10.6 μm. A list of technical specifications is summarised in Table 1. Transverse-mode switching of the laser can be observed through the discolouration of a card (placed approximately one metre from the exit-aperture of the laser). It was found that, although the oscillation can change from one transverse mode to the next, the total output-power remains constant within the resolution of the power-meter (Coherent model 205/201). The transverse modes were found to be predominently TEM_{00} and TEM_{10}.

The laser-discharge tube contains $^{12}CO_2$ and its isotope $^{13}CO_2$. It was therefore necessary to examine the frequency-components of the laser radiation. The radiation, after beam-expansion, was directed into a Perkin-Elmer Fourier-transform interferometer and then analysed. Figure 2 shows the wavelengths at which the laser operates, as given by the F.T.I.R. After an initial stabilisation-time, at which the laser establishes a steady operating-temperature the laser was found to oscillate at wave-lengths of 10.55 μm and 10.61 μm in the intensity-ratio 1:0.733 respectively.

TABLE 1. TECHNICAL SPECIFICATION OF CO_2 LASER

(Model-82-7500-T)

Operational wavelength	10.55 μm and 10.61 μm
Beam diameter ($1/e^2$)	1.5 mm
Beam divergence	8.8 mrad (initially) and 0.44 mrad
Cooling	Convection Air Cooling and temperature stabilised
Input Power	220 VAC at 2.2 A
Output Power	9.05 W continuous
Calculated Rayleigh range	17 cm

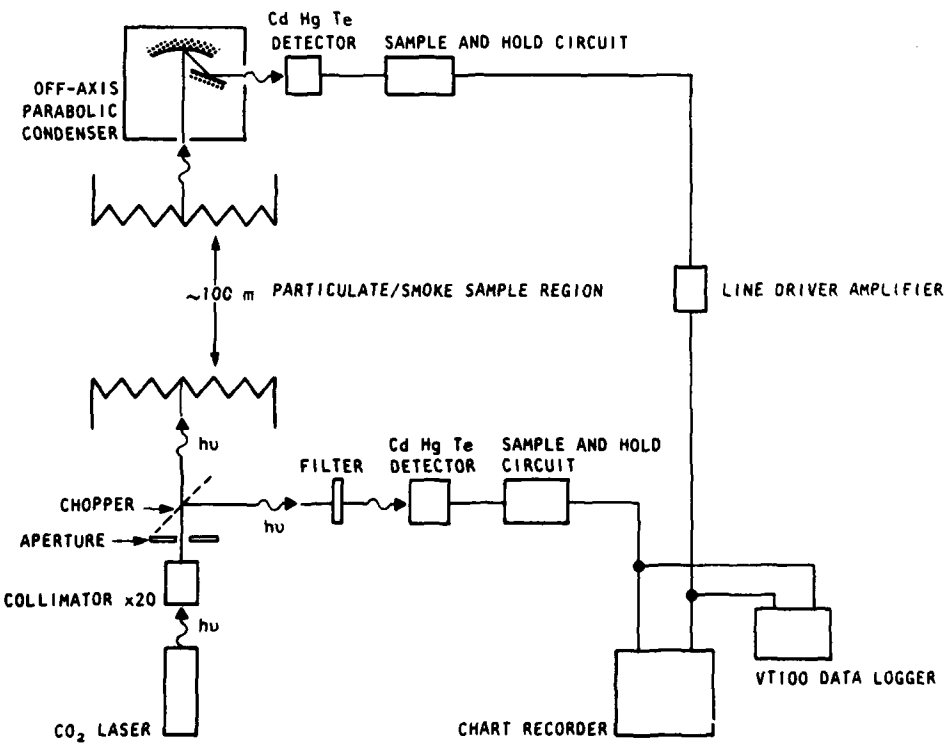

Figure 1. CO_2 Laser Transmissometer showing near- and far-field components. Line drivers are also shown which were used to overcome the voltage drop for cables 100 m or greater in length

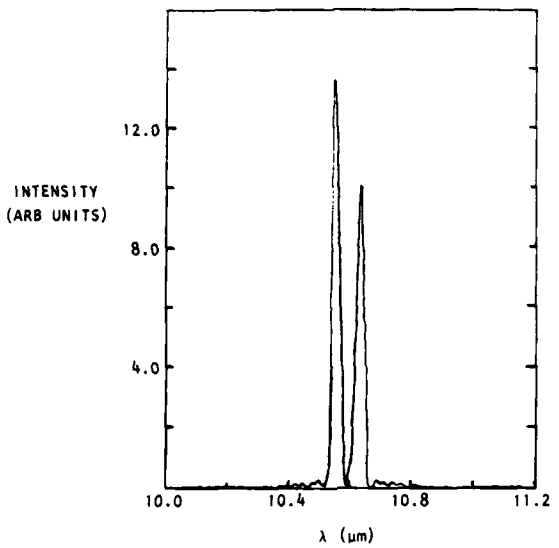

Figure 2. Representing relative intensity of the CO_2 laser oscillating at two distinct wavelengths as measured by the Perkin Elmer FTIR. Other wavelengths of insignificant intensity as compared to the two main 'peaks' are shown in the 'wings' of the structure

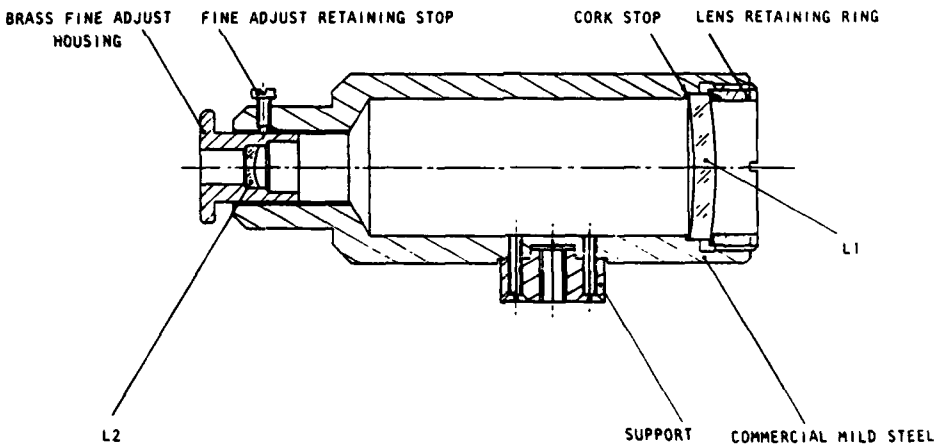

L1 - Germanium exit lens 157.90 mm radius of curvature inside
109.30 mm radius of curvature internal

L2 - Germanium entrance lens, hard carbon-coated,
39.07 mm radius of curvature external
10.95 mm radius of curvature internal

Figure 3. CO_2 laser X20 beam expander illustrating the housed optical components

2.1.2 Beam-expander

The laser-divergence is reduced by x20, so that, at a range of 100 m the spot-diameter ($1/e^2$ of maximum intensity) becomes 4.4 cm. The beam-expander (cf Figure 3) comprises two meniscus germanium lenses of which one is hard carbon coated[1]. The configuration is that of a Galilean telescope-design with a diverging input- and converging output-lens to avoid focussing the beam into a tight waist. The smaller lens is set into a threaded sleeve to allow a fine focussing-adjustment. After the laser-radiation is expanded, it is "apertured" and chopped to produce a modulated signal. As shown in figure 1, the chopper blades are set at 45° to periodically re-direct the radiation to the near-field detector.

2.1.3 Aperture

The beam expander increases the laser beam width from 1.5 mm to a 30 mm diameter beam. Because of the limiting dimensions of the chopper it is necessary to 'aperture' the emerging beam. Chopping of the beam before the beam expander was not successful since at radiation densities of 0.512×10^3 W/cm^2 the low reflectivity of the chopper resulted in a time dependent emissivity.

2.1.4 Detectors

Both the near- and far-field detectors are HgCdTe (Infra-red Associates Inc.) which are cryogenically cooled with liquid nitrogen. The active surface of the detectors are 1 x 1 mm and have a D^* (λ_{pk},10 kHz, 1) of 22×10^9 cm Hz$^{1/2}$/W.

2.2 Far-field components

The far-field components consist of an off-axis parabolic condensor of reflective optics (10 cm diameter primary mirror), and a HgCdTe detector at its focus. The detector was attached to a high-precision XY mount, so that fine adjustments could be made in the horizontal plane. A coarser adjust enabled elevation control.

2.2.1 Recording equipment

A sample-and-hold circuit is used to obtain a DC signal from each detector, by sampling and holding the maximum voltage in the sinusoidal varying signal obtained from modulation by the chopper. The signals are amplified and both recorded on an analogue chart-recorder, and digitised and stored on a 7 channel data-logger. We refer to this as a synchronous detection facility.

2.3 Smoke-particulate analysis

To measure the ability of a smoke or particulate to attentuate laser-radiation, a term defined as the obscuration factor is used, and is represented by the following expression:

$$O_f(t) = 1 - \frac{R(t)-R(o)}{\beta[T(t)-T(o)]}$$

where R(t) represents the signal as a function of time from the far-field detector.

[1] A hard carbon coat is a protective film of carbon which is deposited onto a surface to give it the requisite resilience.

β is a linear gain-factor which, when multiplied by the response of the near-field detector, equals the response as given by the far-field detector.

To further ensure that the smoke or particulate is not self-emitting relative to the laser-intensity, then in the absence of the laser radiation the background signal obtained from the far-field detector should remain unchanged in the presence of the smoke.

2.4 Results

The inclusion of an aperture in the transmissometer was to enable the chopper to completely chop the emerging 3.0 cm diameter laser beam. As stated earlier it would be more beneficial to increase the signal to noise ratio by chopping the laser beam prior to beam expansion with a reflective chopper of low emissivity. The high intensity laser radiation incident on the near field detector would therefore have to be sufficiently attenuated to prevent detector saturation.

An alternative method to increase the signal to noise ratio is to use the laser directly without any collimating optics and place the far field detector at time-invariant points. Again measures must be taken to prevent the near field detector from saturating.

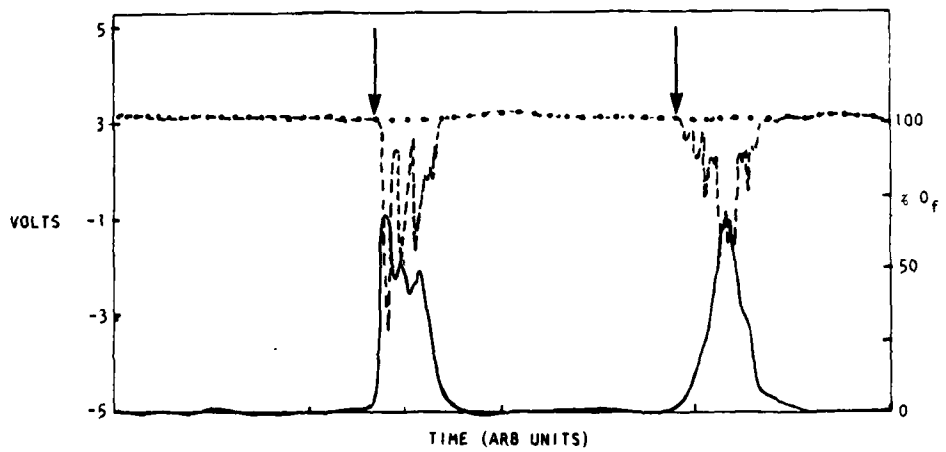

... near field detector signal
— far field detector signal
_ obscuration factor

Figure 4. Curves obtained for near-field and far-field detector signals (upper broken lines). Calculated obscuration factor is also shown (lower solid line). The arrows indicate the time at which aluminium flakes were dispersed across the laser beam

However with the aperture included and as shown (cf Section 3), points of zero or negligible intensity-fluctuation in the far detector plane infer that a detector placed at one of these points should retain a near-constant signal. This was checked prior to the inclusion of particulates between the emitted beam and the far-field detector. Figure 4 shows the near- and far-field detector-response prior and during the introduction of aluminium flakes. Points are indicated on the figure at the time when the flake was introduced, and as shown, the intensity of the received signal became considerably reduced. The solid line represents the temporal obscuration-factor for the particulate, and the vertical axis on the right-hand side indicates the magnitude of obscuration.

Referring to figure 4, the percentage variation (< 5%) in signal prior to intensity attenuation by the aluminium flake, may have arisen from either the signal modulation due to the influence of atmospheric aerosols on the laser beam, or from the time varying points in the neighbourhood of stationary field points of intensity which are simultaneously collected by the parabolic condensor. An evaluation of how extensive are the stationary points could be made by modifying the theoretical equations to allow an integration-ratio over the primary mirror of the condensor rather than a simple ratio as used.

If points to place the detector are indiscriminantly chosen in the far field, the signal variation can become as large as 40%.

3. DIFFRACTION THEORY

Since the laser can oscillate from one TEM mode to a higher one, then indiscriminately placing a detector in a plane perpendicular to the direction of propagation (detector plane) can cause the signal from the detector to vary. Since it is not possible to place the detector at precisely the same amplitude-field point in both the near- and far-fields, then the following technique is used to see if time-invariant point(s) exist(s) in both the diffracted and non-diffracted far-field. The diffracted field is obtained by diffracting the laser beam by an aperture placed in the near field.

3.1 Diffraction Integrals

Several authors have calculated both analytically[1,2] and numerically[3] the near- and far-field diffraction of a plane wave having an intensity profile of the TEM_{00} mode. Higher-order modes can similarly be treated by considering the diffraction integral as follows.

Consider figure 5, which represents the diffraction of a spherical wave through an aperture A. The electro-magnetic field-amplitude at a distance from the aperture is given by[4]

$$U(P) = \frac{-i\varepsilon}{2\lambda} \int_{ap} \frac{[\cos(n,r_0) - \cos(n,s)]}{r_0 S} \exp[-ik(r_0+s)]dS \qquad (1)$$

which is the Fresnel diffraction-integral where λ is the wavelength, ε is a constant of the wave amplitude, k is the propagation number and n is the normal to the Surface defined by the aperture. r and s are the distances between a given point on the aperture surface and the points P_0 and P respectively. If the radius of curvature of the wave at the aperture is large, and P is at a sufficiently large distance from the aperture, then equation (1) becomes

$$U(P) = \frac{C}{r} \int_S \varepsilon(x,y) \exp\left[-ik \frac{(Xx+Yy)}{r}\right] dS \qquad (2)$$

where C is the electro-magnetic field-constant and $\varepsilon(x,y)$ is the electro-magnetic spatial-field variation-term evaluated across the aperture, which depends upon the transverse mode of oscillation within the Laser. If the detector is not at a large range-approximation, then in cylindrical coordinates (and using the small-angle Fresnel approximation[3]) equation (1) becomes (cf. Appendix I)

$$U(X,Y,r) = \frac{C}{r} \int_0^a \rho \exp\frac{(ik\rho^2)}{2r} \int_{-\pi}^{\pi} \varepsilon(\rho,\theta)\exp\frac{-(ik\rho)}{r}\,(X\cos\theta+Y\sin\theta)\, d\theta d\rho \qquad (3)$$

where in the aperture plane $x = \rho\cos\theta$ and $y = \rho\sin\theta$

The term $\varepsilon(\rho,\theta)$ in equations (2) and (3) has a profile dependent upon the laser-mirror geometry.

3.2 Mirror type

For rectangular mirrors, the electro-magnetic field amplitude at the plane of the aperture may be described in terms of Hermite polynomials[5]

ie

$$\varepsilon_{mn}(\rho,\theta) = \varepsilon_o H_m\left(\frac{\sqrt{2}\rho\cos\theta}{\omega}\right) H_n\left(\frac{\sqrt{2}\rho\sin\theta}{\omega}\exp\left(-\left(\frac{\rho}{\omega}\right)^2\right)\right)$$

where

$$H_o(U) = 1;\ H_1(U) = 2U$$

and m and n are the transverse-mode numbers, and ω is the radius of the fundamental mode (m=0,n=0) at 1/e maximum amplitude. $H_a(b)$ is the a^{th} order Hermite polynomial with argument b.

For circular mirrors, the field-amplitude profile at the plane of the aperture can be described in terms of generalised Laguerre polynomials

$$^c\varepsilon_{pq}(\rho,\theta) = {}^c\varepsilon_o\left[\left(\frac{r}{\omega}\right)\sqrt{2}\right]^q L_p^q\left(2\left(\frac{r^2}{\omega^2}\right)\right)\cos q\theta\exp\left(\frac{-r^2}{\omega^2}\right)$$

and

$$L_o^q = 1;\ L_1^q(x) = q+1-x$$

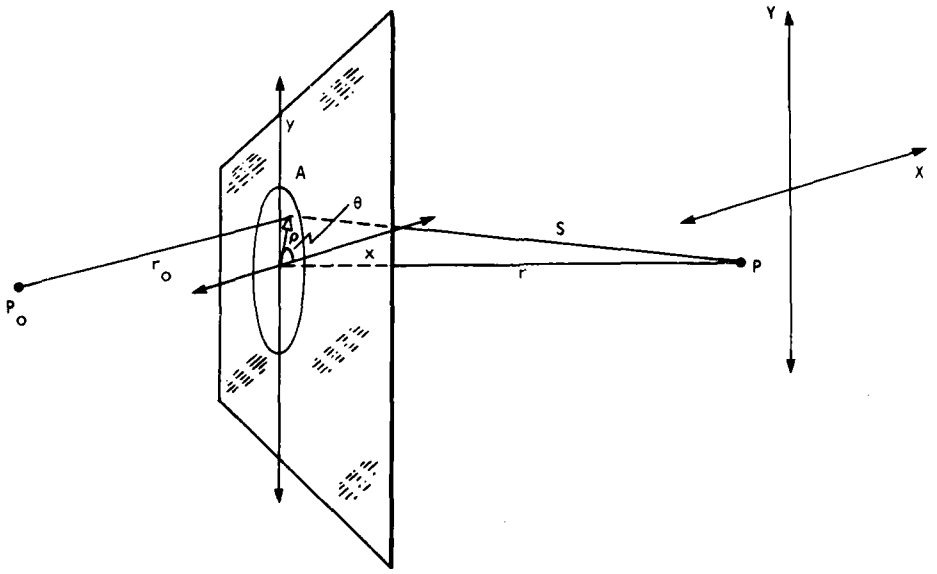

Figure 5. Schematic diagram of diffraction through an aperture. P_o is the point of source for a spherical wave impinging on an aperture A in the xy Plane. r_o is the distance from the point of source to a point in the aperture having coordinates (x,y) or (ρ,θ). s is the distance from this point to a location of observation P in the XY detector plane or observation plane. r is the distance from aperture centre to point P.

Again, p and q describe the mode numbers. Figure 6 shows lower-order amplitudes for both circular and rectangular mirror-configurations. These profiles were numerically calculated on a low-cost "IBM"- PC/XT computer and required 10 K bytes of memory.

Figure 7 shows the profile of the far diffracted intensity distribution obtained from numerically calculating equation (2) by using a 1.5 mm aperture placed in the centre of the collimated beam. The near field electromagnetic field distributions used were for a TEM_{00} and a TEM_{01} wave separately.

3.3 Ratio method

Since we are interested in finding time-invariant points in the detector-plane when the laser oscillates from one transverse mode to the next, then it is instructive to consider the following ratio-definition:

$$R_{mn}^{m'n'} = \frac{I_{m'n'}(X,Y)}{I_{mn}(X,Y)} G_{mn}^{m'n'}$$

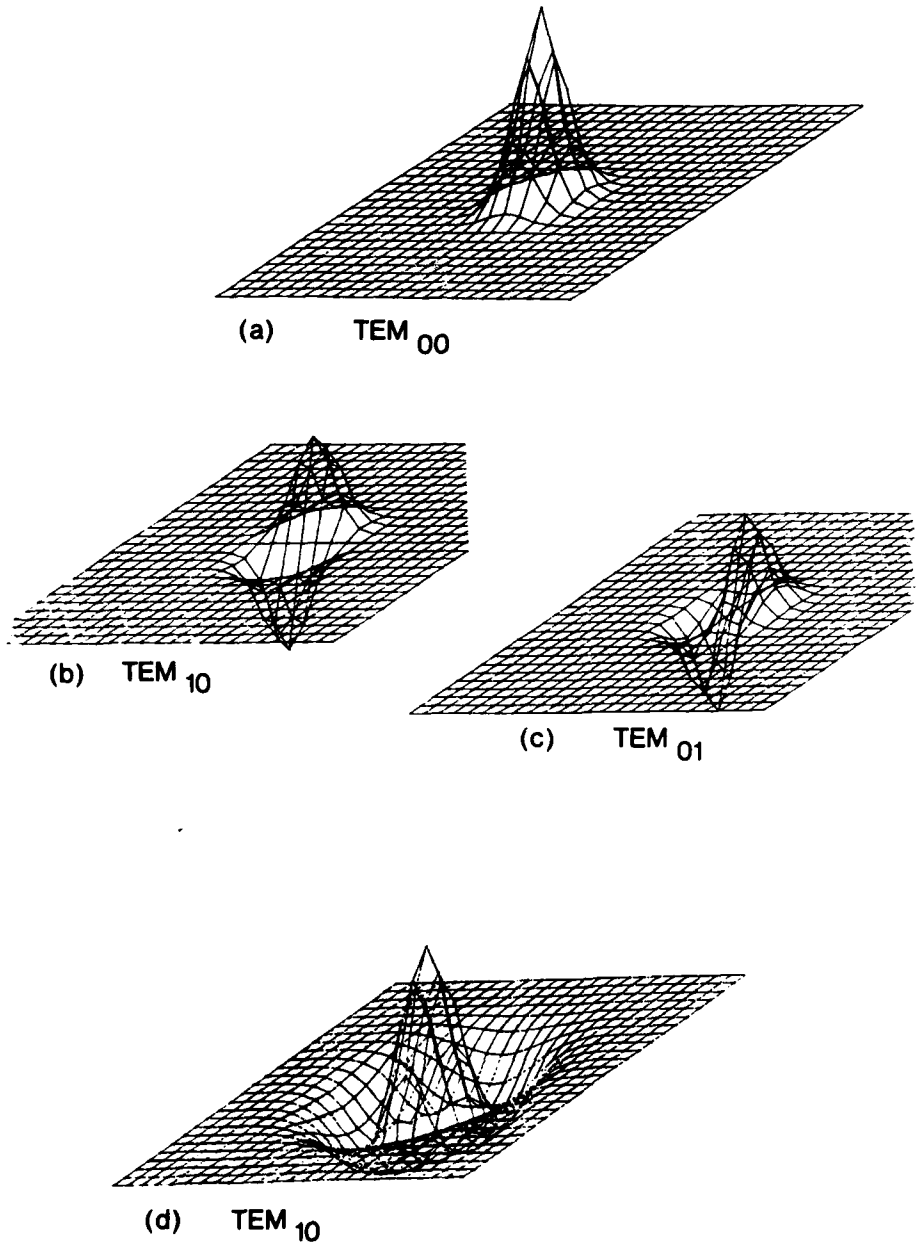

Figure 6. Showing field amplitude profiles for lower order transverse electric modes. (a) and (b) and (c) in addition to rectangle mirrors also apply to circular mirrors (d) is the doughnut distribution for circular mirrors

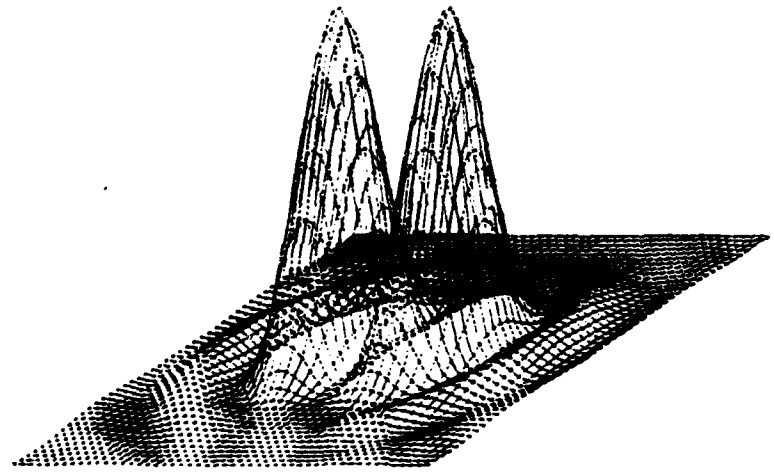

(a) TEM_{00}

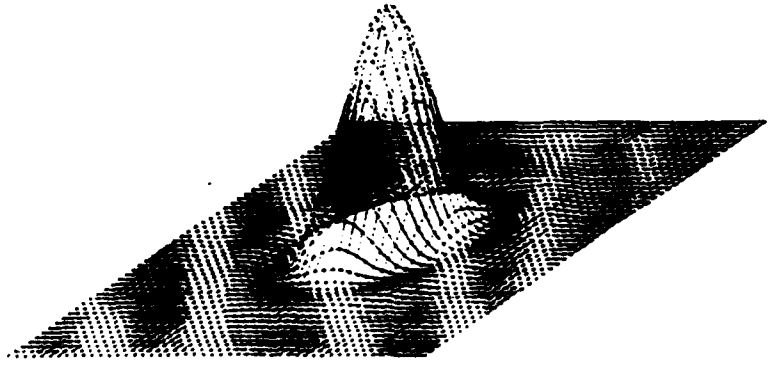

(b) TEM_{01}

Figure 7. Displays of the three dimensional far-field diffracted Intensity distributions for (a) the TEM_{00} mode and (b) the TEM_{01} mode. The beam diameter of the Laser was 30 mm whilst the aperture diameter was 1.5 mm. The distance between the aperture and detector plane was 100 m

where $I_{mn}(X,Y)$ is the intensity of the TEM_{mn} mode. The intensity is found by:

$$I_{mn}(X,Y) = \tfrac{1}{2} U_{mn}(X,Y)\, U^{*}_{mn}(X,Y)$$

U_{mn} is electromagnetic amplitude for the TEM_{mn} mode for the function $\varepsilon(\rho,\theta)$ used in equations (2) or (3) (depending upon the near- or far-field selection). U^{*} is the complex conjugate of U. $G^{m'n'}_{mn}$ is an included coefficient which depends upon which mode-ratio one is considering. It is included to account for conservation of power in the laser-beam cross-section. It has been found that, within the resolution of the power-meter, the total output-power remains constant, after an initial stabilisation-time, when the laser oscillates from one mode to the next,

ie

$$\int_{-\infty}^{\infty} U_{mn}(X,Y)\, U^{*}_{mn}(X,Y)\, dxdy = C_2$$

where C_2 is a constant. As shown in Appendix II, the following values of G are calculated; and for rectangular mirrors

$$G^{00}_{mn} = \begin{cases} 1 & m=o \;\; n=o \\ \frac{1}{2} & m \text{ and } n=o \text{ or } 1 \; m \neq n \\ \frac{1}{4} & m=n=1 \end{cases}$$

Figure 8 is a three-dimensional representation of the amplitude-ratio between the fundamental TEM_{00} mode and the TEM_{10} mode containing one nodal line. To aid interpretation, the numerator is always less than the denominator, by ensuring that

$$R^{m'n'}_{mn} = \frac{I_{m'n'} G^{00}_{mn}}{I_{mn}} \text{ for } I_{m'n'} G^{00}_{mn} \leq I_{mn}$$

$$= \left(\frac{I_{m'n'} G^{00}_{mn}}{I_{mn}} \right)^{-1} \text{ for } I_{m'n'} G^{00}_{mn} > I_{mn}$$

This forces $R^{m'n'}_{mn}$ to be bounded and ≤ 1.

Figure 8 is not scaled and is used as a guide to select regions of maximum amplitude-ratio.

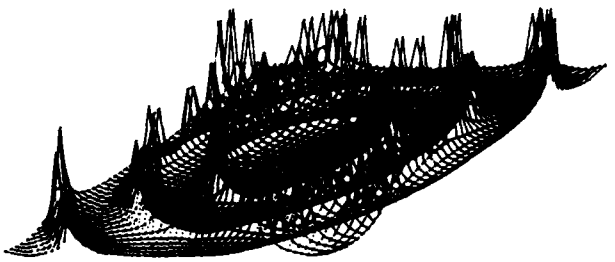

Figure 8. Showing a three dimensional plot of the ratio amplitude

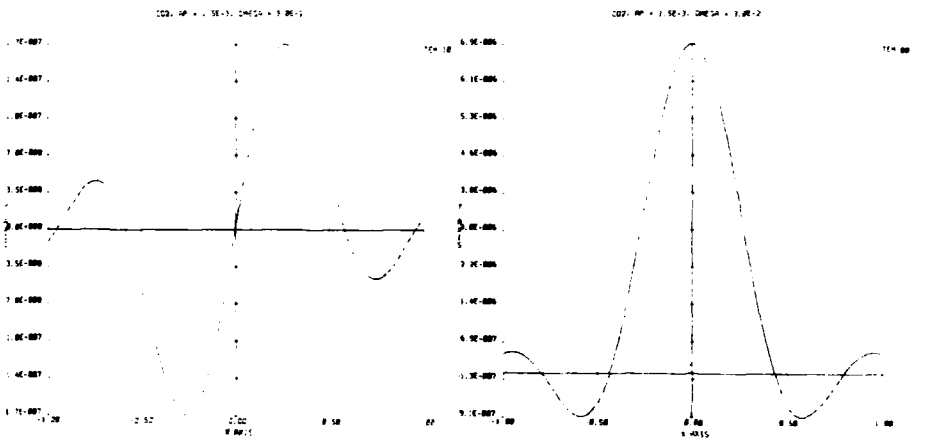

Figure 9. Showing wave amplitude taken down the X axis
(a) Corresponds to TEM_{00} the Gaussian mode whilst
(b) represents the TEM_{10} mode

Note: The near field aperature (1.5 mm in diameter) is placed in the 30 mm diameter laser beam. The electromagnetic field amplitude is at a distance of 100 m from the laser.

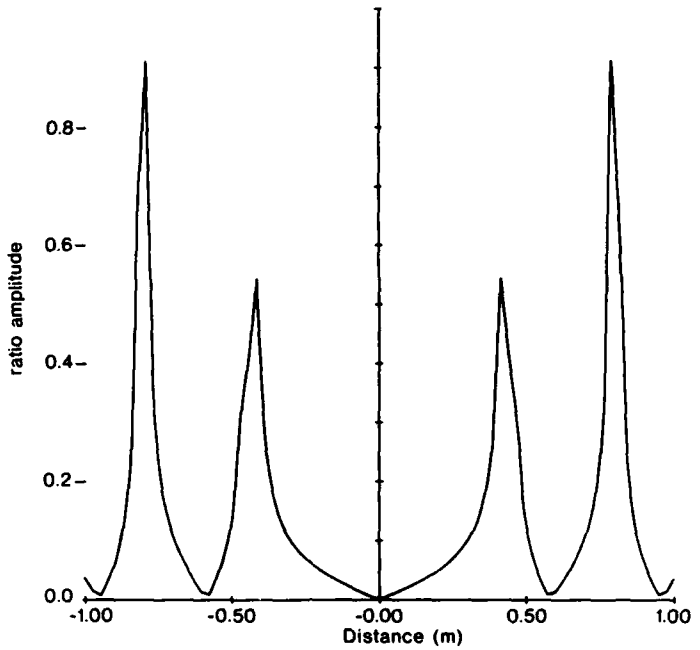

Figure 10. Showing a plot of field amplitude ratio taken down the X axis of figure 8

As shown, the ratio-amplitude has well-defined circular symmetry with maximum values at selected points in the far plane. These maximum points are regions of consideration where points of unity ratio exist, or where local maxima in the intensity exist.

Figure 9 represents the amplitude along the X-axis in the far field for both of the two modes, and figure 10 shows the corresponding two-dimensional ratio. Notice that at a distance of 0.8 m from the centre of the diffracted field, a detector placed at this point would show less than a 10% variation in signal when the laser oscillates between the TEM_{00} and TEM_{01} mode.

4. CONCLUSIONS

Solutions to the diffraction integral in the far field reveal that, when the amplitude-ratio is used, points near and equal to unity exist. A detector placed therefore at these selected points shows minimum fluctuation when the laser oscillates from one lower-order transverse mode to another. For weakly-diffracted far-field distributions, points of unity ratio occur at those azimuth angles as for the undiffracted field.

The laser transmissometer and detector placement-methodology does provide a means to monitor and record 10.6 μm transmissions for smokes and particulates over extended ranges. The synchronous detection facility offers itself for use in regions of highly intense DC sources in the wave-band of concern. A similar treatment of construction and implementation can be applied to lasers operating at other wave-bands such as in the 1 to 5 μm region. Replacement of the CO_2 laser with a tunable laser would offer a diverse narrow-spectral particulate-interrogator over a wide infra-red wave-band.

5. ACKNOWLEDGEMENTS

I would like to thank Mr M. Ritter for his help with programming efforts used in the coding and graphics on the XT computer.

Further, thanks are due to Mr F. Buttignol and Mr J. Wheatley for help with the transmissometer construction.

REFERENCES

No.	Author	Title
1.	Schell, R.G. and Tyras, G.	J. Opt. Soc. Am., 61, 31 (1971)
2.	Belland, P. and Crenn, J.P.	Appl. Opt. 21, 522 (1982)
3.	Campbell, J.P. and DeShazer, L.G.	J. Opt. Soc. Am. 59, 1427 (1969)
4.	Born, M. and Wolf, E.	Principles of Optics, 3rd ed., Ch.8, Pergamon Press, N.Y. (1965)
5.	Smith, P.W.	Proc. IEEE, 58, 1342 (1970)
6.	Smith, W.V. and Sorokin, P.P.	The Laser (McGraw-Hill Book Co. N.Y. 1966) Ch.2
7.	Kogelnik, H. and Li, T.	Laser Beams and Resonators, Laser Theory (ed. Frank S. Barnes) IEEE Press, N.Y. 1972

APPENDIX I

DIFFRACTION INTEGRAL IN THE NEAR-FIELD

Taking the approach of Campbell and Deshazzar[3] and with reference to figure 5, then the Kirchoff diffraction-integral for an aperture illuminated by a normal-incident plane wave is given by

$$U(X,Y,r) = C\ \varepsilon(x,y)\ \frac{(1+\cos\beta)}{s}\ \exp[iks]dxdy \qquad (I.1)$$

where the term $(1+\cos\beta)$ is the obliquity factor,
C is a constant,
s is the distance from a point (x,y) in the aperture -plane to any given point in the detector-plane,
k is given by $(2\pi/\lambda)$.

The distance s is given by

$$s^2 = Z^2 + (X-x)^2 + (Y-y)^2$$

where Z is the distance between the aperture centre and observation plane centre, and

$$r^2 = X^2 + Y^2 + Z^2$$

or

$$s^2 = r^2 + (x^2+y^2) - 2(Yy+Yx)$$

letting

$$\rho^2 = x^2+y^2;\ x = \rho\cos\theta \text{ and } y = \rho\sin\theta$$

then

$$s = r\left[1 + \frac{\rho^2}{r^2} - \frac{2\rho}{r^2}\ (X\cos\theta + Y\sin\theta)\right]^{\frac{1}{2}}$$

Expanding this into a Taylor series around unity, we have

$$s = r + \frac{\rho}{r}(X\cos\theta + Y\sin\theta) + \frac{1}{2}\frac{\rho^2}{r}\left(1 + \frac{(X\cos\theta + Y\sin\theta)^2}{r^2}\right)$$

$$-\frac{1}{2}\frac{\rho^3}{r^2}(X\cos\theta + Y\sin\theta)\left(1 + \frac{(X\cos\theta + Y\sin\theta)^2}{r^3}\right) + \ldots.$$

With the Fresnel and small-angle approximations, then:

$$s \cong r + \frac{\rho}{r}(X\cos\theta + y\sin\theta) + \frac{1}{2}\frac{\rho^2}{r}$$

Equation (1) becomes

$$U(X,Y,r) = \frac{C'}{r}\int_0^a \rho \exp\left(\frac{ik\rho^2}{2r}\right)\int_0^{2\pi} \varepsilon(r,\theta)\exp\left(-\frac{ik\rho}{r}(X\cos\theta + y\sin\theta)\right)d\theta d\rho$$

APPENDIX II

RATIO CONSTANTS

To evaluate the ratio-constants as described on page 8, the power in the laser field at the aperture, prior to diffraction by the aperture, is derived for the first two transverse electro-magnetic modes.

TEM_{00}: For the first transverse mode, the power in the field for rectangular laser mirrors is given by

$$I_{00} = \int_S \frac{1}{2} U(\rho,\theta)\, U^*(\rho,\theta) dS$$

where

$$U(\rho,\theta) = \varepsilon_0 H_0 H_0 \exp\left(-\frac{(x^2+y^2)}{\omega^2}\right)$$

thus

$$I_{00} = \frac{\varepsilon_0^2}{2} \int_{-\infty}^{\infty} \int_{-\infty}^{\infty} \left(H_0\, H_0 \exp\left(-\frac{(x^2+y^2)}{\omega^2}\right)\right)^2 dxdy$$

$$= \frac{\varepsilon_0^2}{2} \left[\frac{\sqrt{\pi\omega}}{\sqrt{2}}\right]\left[\frac{\sqrt{\pi\omega}}{\sqrt{2}}\right]$$

$$= \varepsilon_0^2\, \pi\omega^2/4$$

TEM_{10} For the 1, 0 transverse mode, the power in the field is given by

$$I_{10} = \varepsilon_0^2 \int_{-\infty}^{\infty} \int_{-\infty}^{\infty} \frac{x^2}{\omega^2} \exp\left(-\frac{2}{\omega^2}(x^2+y^2)\right) dy\, dx$$

$$= \frac{\varepsilon_0^2}{\omega^2} \left[\frac{1}{2}\, \frac{\omega^2}{2}\, \frac{\sqrt{\pi\omega}}{\sqrt{2}}\right]\left[\frac{\sqrt{\pi\omega}}{\sqrt{2}}\right]$$

$$= \varepsilon_o^2 \omega^2 \pi/8$$

therefore for rectangular mirrors, since by definition

$$G_{mn}^{m'n'} = R_{mn}^{m'n'} I_{mn}(x,y)/I_{m'n'}(x,y)$$

$$G_{mn}^{oo} = \begin{cases} 1 & 00 \\ \frac{1}{2} & 01 \text{ or } 10 \\ \frac{1}{4} & 11 \end{cases}$$

For the case with circular laser mirrors, the intensity of the field is given by

$$I_{pq} = \int_0^{2\pi} \int_0^{\infty} \frac{\rho}{2} U_{pq}(\rho,\theta) U_{pq}^{*}(\rho,\theta) \, d\rho \, d\theta$$

Again for TEM_{00} mode

$$I_{oo} = \pi \varepsilon_o^2 \int_0^{\infty} \rho \exp(-2\rho^2/\omega^2) \, dr$$

$$= \pi \omega^2 \varepsilon_o^2/4$$

which is identical with that of the rectangular mirror case.

The TEM_{01} mode distribution is identical with the rectangular case. The TEM_{10} distribution is called the "doughnut mode", the power in which is given by

$$I_{10} = \int_0^{\infty} \int_0^{2\pi} \rho \frac{\varepsilon_o^2}{2} (1-2(\rho^2/\omega^2))^2 \exp(-2\rho^2/\omega^2) \, d\theta d\rho$$

by change of variables

$$= \pi \varepsilon_o^2 \int_{-1}^{\infty} u^2 \exp(-(1+u))\, \omega^2\, du$$

$$= \pi \varepsilon_o^2 \omega^2 / 4$$

so, for circular mirrors, we have

$$G_{mn}^{oo} = \begin{cases} 1 & 00 \\ 1 & 10 \text{ doughnut} \\ \frac{1}{2} & 01 \text{ and } 11 \end{cases}$$

DISTRIBUTION

	Copy No.
DEPARTMENT OF DEFENCE	
Defence Science and Technology Organisation	
Chief Defence Scientist Assistant Chief Defence Scientist (Policy) Assistant Chief Defence Scientist (Operations) Director General External Relations Director General Science Technology Programs	1
Counsellor, Defence Science, London	Cnt Sht Only
Counsellor, Defence Science, Washington	Cnt Sht Only
Counsellor, Defence Science, Bangkok	Cnt Sht Only
Scientific Attache to Defence Research Centre, Kuala Lumpur	Cnt Sht Only
Electronics Research Laboratory	
Director, Electronics Research Laboratory	2
Superintendent, Electronic Warfare Division	3
Superintendent, Optoelectronics Division	4
Senior Principal Research Scientist, Electronic Warfare Division	5
Principal Officer, Optical Electronic Warfare Group	6
Principal Officer, Optical Development Group	7
Principal Officer, Electronic Warfare Techniques Group	8
Principal Officer, Sensing and Propagation Group	9
Dr S. S. Ti, Optical Electronic Warfare Group	10
Dr T. Moon, Optical Electronic Warfare Group	11
Mr R. J. Oermann, Optical Electronic Warfare Group	12
Mr O. Scott, Optical Electronic Warfare Group	13
Advanced Engineering Laboratory	
Director, Advanced Engineering Laboratory	14

DOCUMENT CONTROL DATA SHEET

Security classification of this page : UNCLASSIFIED

1 DOCUMENT NUMBERS

AR Number : AR-004-991

Series Number : ERL-0426-TR

Other Numbers :

2 SECURITY CLASSIFICATION

a. Complete Document : Unclassified

b. Title in Isolation : Unclassified

c. Summary in Isolation : Unclassified

3 DOWNGRADING / DELIMITING INSTRUCTIONS

4 TITLE

CO_2 (10.6 μm) LASER TRANSMISSOMETER

5 PERSONAL AUTHOR (S)

S.A. Brunker

6 DOCUMENT DATE

September 1987

7 7.1 TOTAL NUMBER OF PAGES 19

7.2 NUMBER OF REFERENCES 7

8 8.1 CORPORATE AUTHOR (S)

Electronics Research Laboratory

8.2 DOCUMENT SERIES and NUMBER
Technical Report
0426

9 REFERENCE NUMBERS

a. Task : AIR 86/304

b. Sponsoring Agency :

10 COST CODE

136

11 IMPRINT (Publishing organisation)

Defence Science and Technology Organisation Salisbury

12 COMPUTER PROGRAM (S) (Title (s) and language (s))

13 RELEASE LIMITATIONS (of the document)

Approved for Public Release

Security classification of this page : UNCLASSIFIED

Security classification of this page : UNCLASSIFIED

14 ANNOUNCEMENT LIMITATIONS (of the information on these pages)

No limitations

15 DESCRIPTORS

a. EJC Thesaurus Terms

Transmissometers
Continuous wave lasers
Diffraction analysis

b. Non - Thesaurus Terms

16 COSATI CODES

0046C

17 SUMMARY OR ABSTRACT
(if this is security classified, the announcement of this report will be similarly classified)

A commercially-obtained CO_2 California continuous-wave (c.w.) laser was used as the infrared (I.R.) emitting component in the construction of a 10.6 μm Laser Transmissometer. This report describes the construction and establishes the performance of the transmissometer. It was found that the laser would oscillate unpredictably between the lower-order transverse electro-magnetic modes, and it was therefore necessary to try to predict pseudo-stationary points in the far diffracted field.

Security classification of this page : UNCLASSIFIED